Vesta I. Bateman
William B. Leisher
Fred A. Brown
Neil T. Davie
Sandia National Laboratories
Albuquerque, NM 87185

Calibration of a Hopkinson Bar with a Transfer Standard

A program requirement for field test temperatures that are beyond the test accelerometer operational limits of −30°F and +150°F required the calibration of accelerometers at high shock levels and at the temperature extremes of −50°F and +160°F. The purposes of these calibrations were to insure that the accelerometers operated at the field test temperatures and to provide an accelerometer sensitivity at each test temperature. Because there is no National Institute of Standards and Technology traceable calibration capability at shock levels of 5,000–15,000 g for the temperature extremes of −50°F and +160°F, a method for calibrating and certifying the Hopkinson bar with a transfer standard was developed. Time domain and frequency domain results are given that characterize the Hopkinson bar. The National Institute of Standards and Technology traceable accuracy for the standard accelerometer in shock is ±5%. The Hopkinson bar has been certified with an uncertainty of 6%.

INTRODUCTION

The theory of stress wave propagation in a Hopkinson bar is well documented in the literature (Davies, 1948; Kolsky, 1953). The results of this theory are summarized as follows. A Hopkinson bar is defined as a perfectly elastic, homogeneous bar of constant cross-section. A stress wave will propagate in a Hopkinson bar as a one-dimensional elastic wave without attenuation or distortion if the wavelength, λ, is large relative to the diameter, D, or $10D \leq \lambda$. For a one-dimensional stress wave propagating in a Hopkinson bar, the motion of a free end of the bar as a result of this wave is:

$$v = 2c\varepsilon \tag{1}$$

or

$$a = 2c\left[\frac{d\varepsilon}{dt}\right] \tag{2}$$

where v and a are the velocity and acceleration, respectively, of the end of the bar, $c = \sqrt{E/\rho}$ is the wave propagation speed in the bar, E is the modulus of elasticity, ρ is the density for the Hopkinson bar material, and ε is the strain measured in the bar at a location that is not affected by reflections during the measurement interval.

The motion of an accelerometer mounted on the end of the bar will be governed by Eq. (1) and (2) if the mechanical impedance of the accelerometer is much less than that of the bar or if the thickness of the accelerometer is much less than the wavelength. The requirement on the strain gage is that the gage length (g.l.) be less than the wavelength or $\lambda \geq 10$ g.l.

The Shock Laboratory Hopkinson bar, used for accelerometer testing, is shown schematically in Fig. 1 and is made of 6 Al, 4 V titanium alloy (6% aluminum and 4% vanadium) with a 72-in. length and a 0.76-in. diameter. The bar is supported in a way that allows it to move freely in the axial direction. A low pressure air gun is used to fire a 2-in. long hardened tool steel projectile at the end of the bar. This impact creates a stress

Shock and Vibration, Vol. 1, No. 2, pp. 145–152 (1993)

CCC 1070-9622/93/020145-08

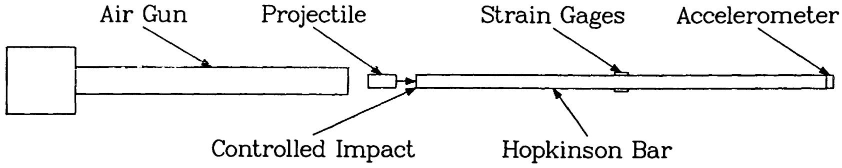

FIGURE 1 Hopkinson bar configuration.

pulse that propagates toward the opposite end of the Hopkinson bar. The amplitude of the pulse is controlled by regulating the air gun pressure, which determines the impact speed. The shape (approximately a half sine) and duration of the pulse are controlled by placing various thicknesses of paper (3 × 5 index cards) on the impact surface. The two strain gages are located 49.75 in. from the end on which the accelerometer is mounted and are mounted at diametrically opposite positions on the bar. The 49.75-in. strain gage location is in the mid-portion of the bar and allows a longer incident pulse, if desired. These gages are connected in opposite arms of a Wheatstone bridge in order to measure the net axial strain.

Once recorded, the strain and acceleration records can be compared by using either velocity or acceleration as shown in Eqs. (1) and (2). When these comparisons are made, the time delay of the acceleration record, which is equal to the time for the wave to propagate from the strain gage to the end of the bar, must be taken into account. Hopkinson bar accelerometer calibration methods documented in the literature (Cannon and Rimbey, 1971; Brown, 1963; Sill, 1983) generally use velocity, in which case the accelerometer record is integrated and compared directly to the strain record converted to velocity by the factor $2c$. This provides smooth curves for comparison of time histories; however, much of the higher frequency information is lost due to the integration process. Because we wanted to preserve the frequency response of the data, acceleration was used for the comparison of the data. Consequently, the time derivative of the strain records was required, and the resulting signal may be contaminated by high frequency noise created in the process of calculating the derivative. This problem was essentially eliminated by: adequate sample rate of 500 kHz or higher; low pass digital filtering with a cutoff frequency well above the frequency range of interest (10 kHz); and most importantly, an accurate differentiation algorithm that was derived using the Fourier series reconstruction techniques of Stearns (1978). This algorithm results in an exact derivative of the digitized signal providing the Sampling Theorem has not been violated, that is, the data is not aliased (Stearns, 1975).

The selected technique for calculating the sensitivity change at temperatures other than ambient, using the acceleration derived from the Hopkinson bar strain measurements, can be used only to estimate the change in sensitivity due to temperature because of the uncertainties associated with the measurements. Most of the errors are deterministic and will be cancelled when the percentage sensitivity change due to the $-50°F$ temperature is calculated in the equation (Bateman, Leisher, Brown, and Davie, 1991):

$$C = \left[\frac{A_{\text{Ac-50}}}{A_{\text{Ac-A}}} \cdot \frac{A_{\text{Hop-A}}}{A_{\text{Hop-50}}} - 1\right] \times 100 \qquad (3)$$

where C = percentage sensitivity change at $-50°F$ as compared to ambient; $A_{\text{Ac-50}}$ = shock amplitude measured by the accelerometer at $-50°F$; $A_{\text{Ac-A}}$ = shock amplitude measured by the accelerometer at ambient; $A_{\text{Hop-A}}$ = shock amplitude derived from strain gages for ambient test; and $A_{\text{Hop-50}}$ = shock amplitude derived from strain gages for $-50°F$ test. A similar equation is used for the sensitivity change at $+160°F$.

The Hopkinson bar has been used to test accelerometers at the temperatures of $-50°F$ and $+160°F$. The purpose of these tests has been twofold. Because the specified operational temperature for these accelerometers is $-30°F$ to $+150°F$, the Hopkinson bar tests are intended as screening tests to increase the probability that the accelerometers will not fail at the field test temperatures of $-50°F$ and $+160°F$. A failure rate of 12% (11 out of 93 failed) has been observed at these temperatures (Bateman et al., 1991). An accelerometer fails if it has a large sensitivity deviation or if it breaks. A second purpose of the Hopkinson tests is to calculate a sensitivity change for the accelerometers with the strain gages on the bar as a reference measurement. Sensitivity changes are on the order of 5–10% at these temperatures and agree well with the manufacturer's specifications. A calibration of the Hopkinson bar was performed for documentation purposes and consisted of three different evaluations. First, a calculation of the wave speed for the titanium Hopkinson bar was made at the temperatures of −50°F and +160°F. Second, a standard accelerometer, calibrated by the National Institute of Standards and Technology traceable (NIST-traceable) standards, was placed on the end of the bar in the same manner as the accelerometers for the calibration tests and was subjected to shock pulses at various amplitudes. The standard accelerometer output was compared to the acceleration calculated from the Hopkinson bar strain gage response. Last, a static load test was performed on the Hopkinson bar, and an effective gage factor was calculated from the measured bar sensitivity.

RESULTS

The stress wave speed in the Hopkinson bar is an important quantity because it occurs in the Hopkinson bar acceleration calculation as shown in Eqs. (1) and (2). The stress wave speed is calculated from material properties as:

$$c = \sqrt{\frac{E}{\rho}} \tag{4}$$

where E is the modulus of elasticity and ρ is the density for the Hopkinson bar material. The modulus varies between 102% at −50°F and 97% at +165°F of the nominal value, 16×10^6 psi (*Metallic Materials and Elements for Aerospace Vehicle Structures,* 1987). The change in density is 0.0015% at either of the temperature extremes and is negligible (*Metallic Materials and Elements for Aerospace Vehicle Structures,* 1987). The nominal stress wave speed for titanium is 196,210 in./s. At the cold temperature, the wave speed will increase by $\sqrt{1.02}$ or 1.00995 (1%) in the length of the bar that is inside the temperature chamber, about 2 in. Because the round trip time to the strain gages is measured for the stress wave speed, the stress wave travels twice that distance or 4 in. at about 5 μs/in. It takes 20 μs for the stress wave to traverse this distance. An upper bound for the increase in this time due to the cold temperature is 1% of 20 μs or 0.2 μs. Because the highest resolution available with Shock Laboratory instrumentation is 0.5 μs, this increase in the stress wave speed cannot be measured at −50°F. A similar argument can be made for the decrease in wave speed at the hot temperature; the decrease is about 2% over the 4-in. bar length or 0.4 μs. Again, this change in the wave speed will not be detected with current instrumentation time resolution. These calculations were verified with Hopkinson bar measurements, and consequently, the stress wave speed was not changed for accelerometer calibrations performed at −50°F or +160°F.

A standard accelerometer was used for the second part of the Hopkinson bar evaluation. The standard accelerometer has a NIST-traceable calibration for both shock and vibration. The standard accelerometer was placed on the Hopkinson bar in Fig. 1 in the same manner as the accelerometers calibrated. The response of the standard accelerometer was compared to the acceleration derived from the strain gages on the bar using a frequency response function. For a nominal pulse duration of 100 μs and three shock levels (4,000, 10,000, and 15,000 g), an ensemble of five pulses was applied to the standard accelerometer. Examples of each shock pulse with its corresponding Fourier transform magnitude measured by the strain gages are shown in Figs. 2–4. Considerable preparation of the Hopkinson Bar data was required before frequency response functions could be calculated. Because an acceleration response to the acceleration input frequency response function was desired, the strain data was converted to velocity according to Eq. (1). The velocity data were digitally filtered with a 10-pole Butterworth filter whose cutoff frequency of 17 kHz was chosen to reduce the noise created in taking the derivative to obtain the acceleration. The data were filtered in both the forward and backward directions to remove the filter phase shift. The 17-kHz cutoff frequency was determined from an examination of the Fourier transform magnitude. The cutoff frequency for the filter was chosen based on two criteria: the frequency at which the pulse transform becomes noise and the frequency at which the coherence, computed using an ensemble average, between the input and response accelerations deviated from unity. The filter cutoff frequency was chosen higher than the second frequency so that the filter attenuation did not affect the coherent frequency range. Input acceleration was calculated by taking the derivative of the velocity as described in the previous section.

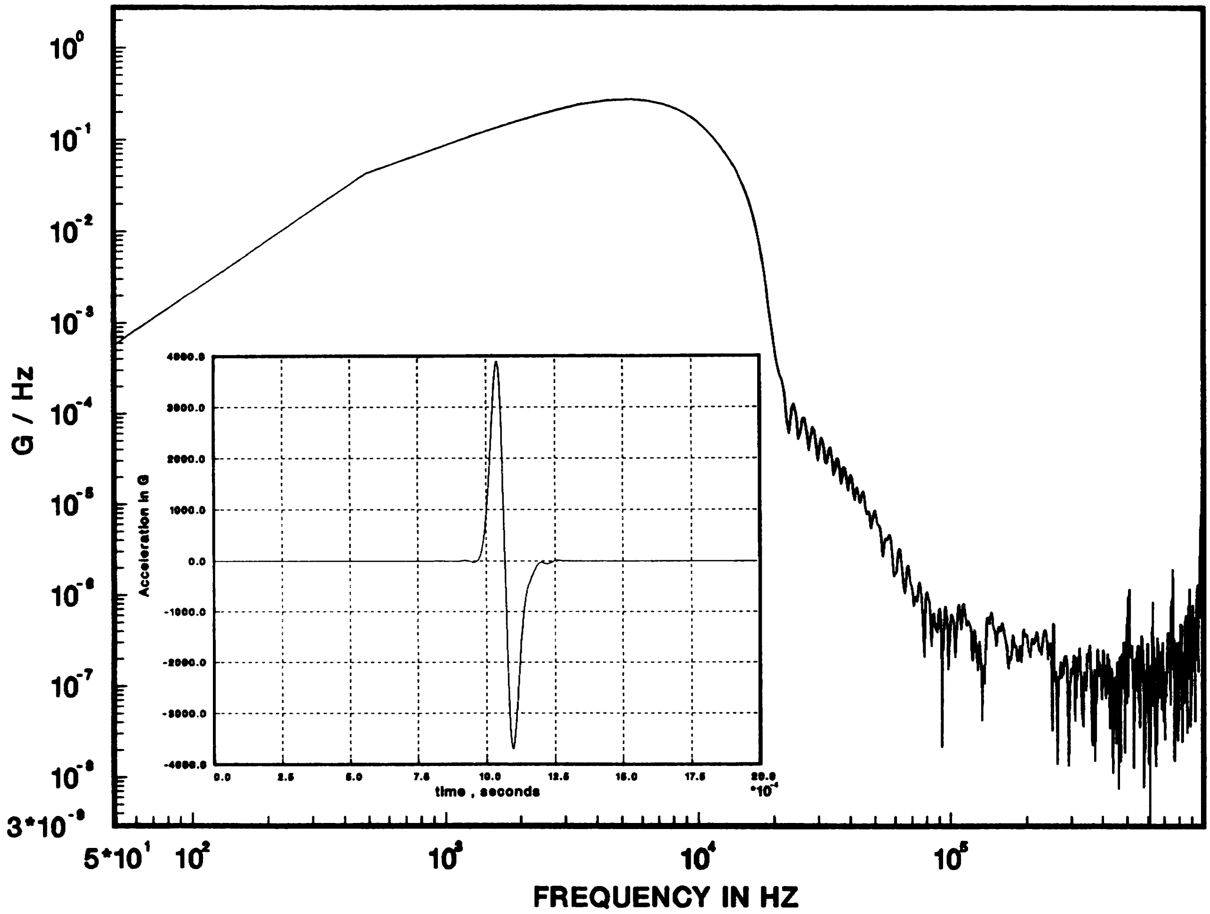

FIGURE 2 Fourier transform magnitude for 4,000 g pulse.

The resultant input acceleration was then shifted in time to account for the wave transit time from the strain gage to the accelerometer assembly. Several tests were performed to determine the correct time shift measured as 261 μs. This value is one-half the time for the stress wave to travel to the end of the bar and back to the strain gages. The resulting input acceleration data as well as the response data were filtered at 40 kHz with a 10-pole Butterworth digital filter in both a forward and backward directions to eliminate filter phase shift and then windowed. A boxcar window tapered with Blackman–Harris cosine functions was applied to prevent leakage errors. The effects of the window and the filter were examined closely to assure that they did not produce any contamination of the data.

The magnitude and phase of the frequency response functions, with Hopkinson bar as input and the standard accelerometer as output, were calculated so that a quantitative evaluation could be made of the Hopkinson bar as compared to the standard accelerometer. The input acceleration pulse and the accelerometer response data were used to calculate a transfer function, $H(j\omega)$, using the following equations (Bendat and Piersol, 1986),

$$H(j\omega) = \frac{H_1(j\omega) + H_2(j\omega)}{2}$$

where,

$$H_1(j\omega) = \frac{\Sigma G_{xy}(j\omega)}{\Sigma G_{xx}(j\omega)} \quad \text{and} \quad H_2(j\omega) = \frac{\Sigma G_{yy}(j\omega)}{\Sigma G_{yx}(j\omega)} \tag{5}$$

and where G_{xy} is the cross-spectrum between the input acceleration pulse measured on the Hopkinson bar and the measured accelerometer response; G_{yx} is the cross-spectrum between the response and the input; G_{yy} is the auto-spectrum of the response; and G_{xx} is the auto-spectrum of the input. The averaging operation for $H(j\omega)$ is

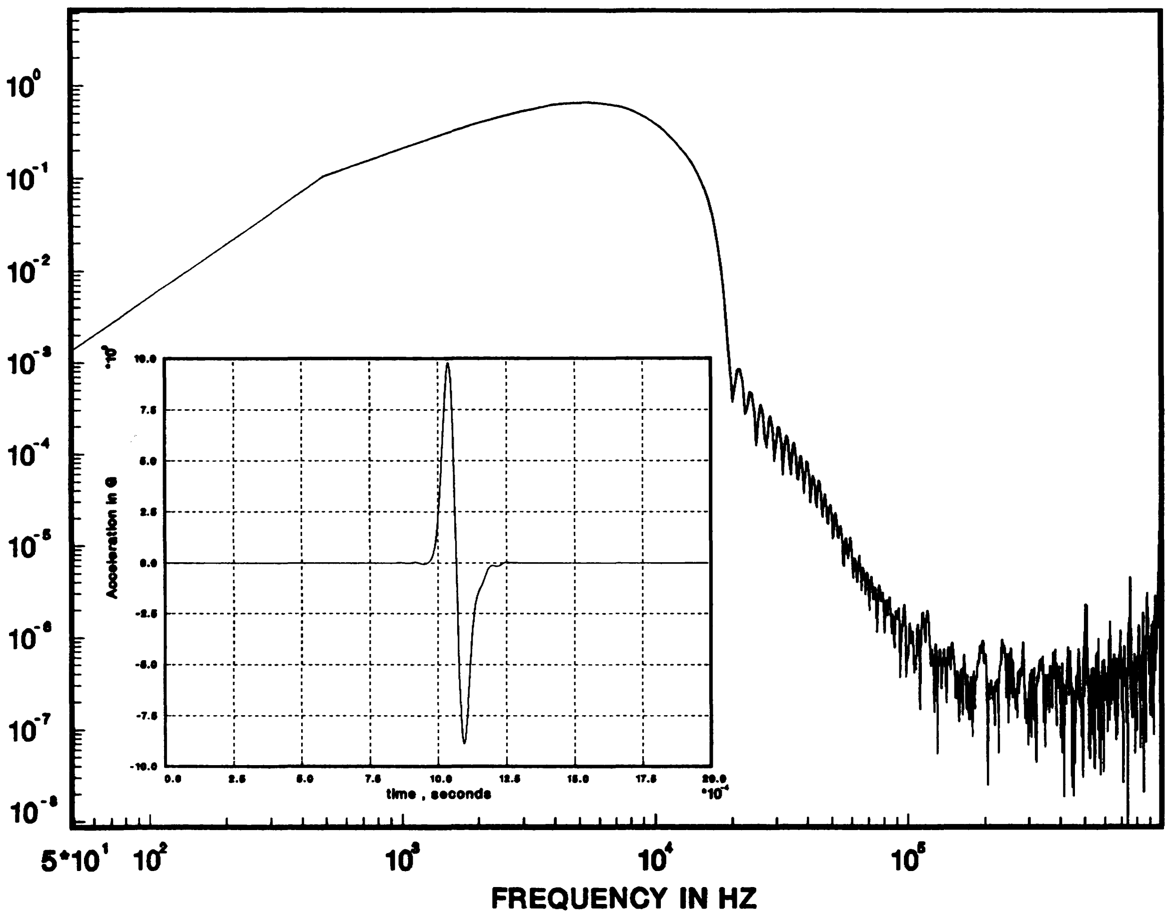

FIGURE 3 Fourier transform magnitude for 10,000 *g* pulse.

acceptable if the noise is small and if the input and output have similar magnitudes. The functions H_1 and H_2 have different characteristics in general. The frequency response function, H_1, is biased by the error on the input, and the frequency response function, H_2, is biased by the error on the output. In the case of the Hopkinson bar data, there was noise on both the input and the output, so the average of the two frequency response functions H_1 and H_2 was used. The summations are performed for the ensemble of five shock pulses input to the accelerometer at a particular shock level and pulse duration. The coherence, $\gamma^2_{xy}(j\omega)$, was also calculated for an ensemble of data for a set of conditions according to the equation (Bendat and Piersol, 1986).

$$\gamma^2_{xy}(j\omega) = \frac{H_1(j\omega)}{H_2(j\omega)} \qquad (6)$$

as a measure of the linearity between the input as calculated from the Hopkinson bar strain data and the accelerometer response output and of the noise in the input and the response data. The coherence was greater than 0.99 in all cases.

The frequency response functions for the three different acceleration inputs are shown in Fig. 5. Also shown in Fig. 5 is the variation of the standard accelerometer sensitivity as a function of frequency. Each curve is plotted as percent difference from the 1000-Hz value for that curve. The 1000-Hz value was chosen because of noise problems at lower frequencies. The maximum deviations of the Hopkinson bar frequency response functions from the standard accelerometer curve are -1% and $+5\%$ at 10 kHz.

A static force calibration to determine the effective gage factor of the titanium bar was undertaken as the last part of the certification effort. The bar was placed vertically in a load test machine (manufactured by MTS) and was loaded with a 500-lb. compressive load in 50-lb. increments. The output of the strain gages was compared to a NIST-traceable calibrated load cell,

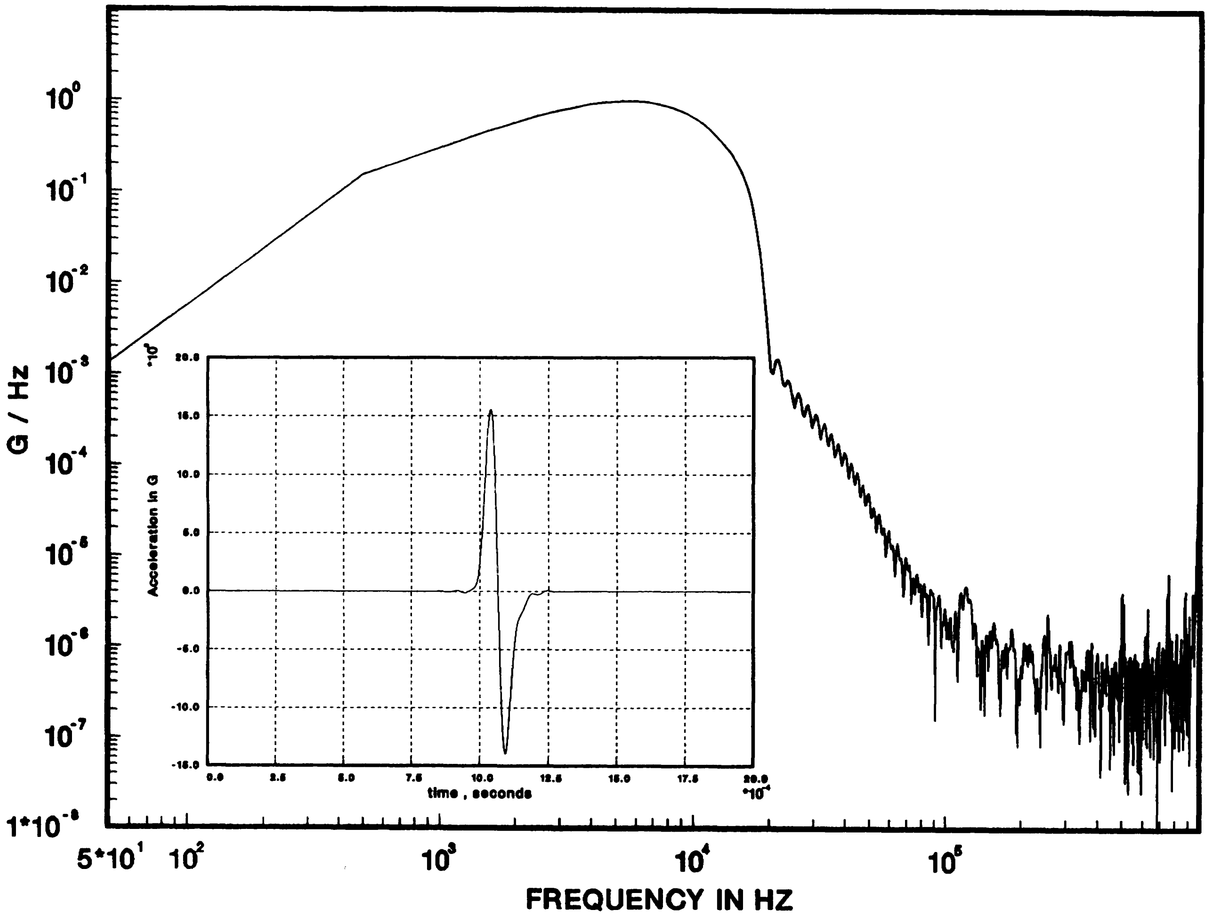

FIGURE 4 Fourier transform magnitude for 15,000 g pulse.

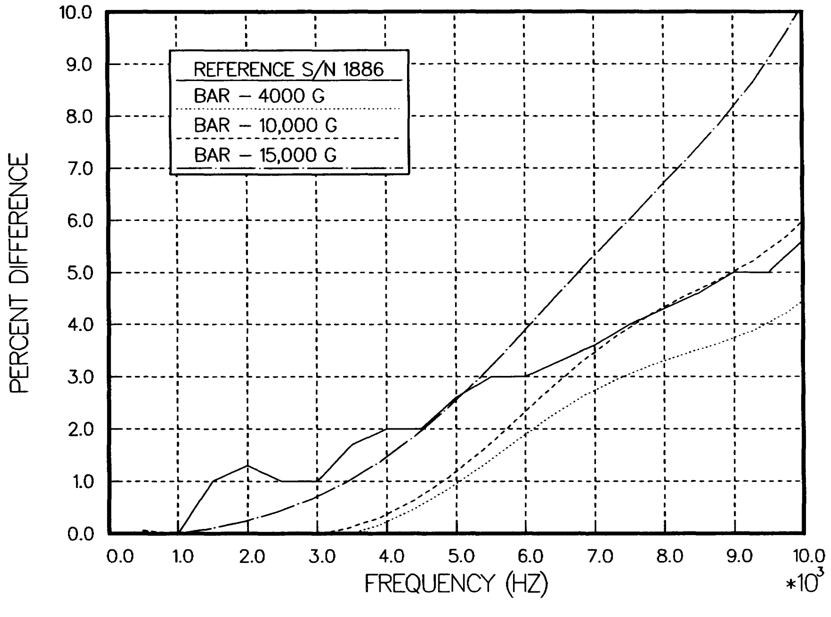

FIGURE 5 Reference accelerometer and Hopkinson bar Frequency Response Functions.

and a sensitivity for the strain gage, S_{sg}, was calculated in $\mu v/v/\text{lb}$. The indicated force, F_1, from the bar is then:

$$F_1 = \frac{V_{out}}{S_{sg} V_e} \tag{7}$$

where V_{out} is the output voltage from the strain gages as the load is applied and V_e is the excitation voltage on the strain gage bridge. This force, F_1, may be compared to the force measured on the bar, F_2, in response to a shock pulse:

$$F_2 = \frac{2EAV_{out}}{G_f V_e} \tag{8}$$

where G_f is the gage factor, E is the modulus of elasticity, and A is the bar cross-sectional area. F_1 and F_2 are set equal to each other in order to calibrate the output F_2. After common quantities are cancelled, th equality becomes an expression for an equivalent gage factor as:

$$G_f = 2 \cdot E \cdot A \cdot S_{sg} \tag{9}$$

that has a numerical value of 2.07. This value is 3% lower than the manufacturer's specified value of 2.135. An examination of the numerical values for the frequency response functions, instead of the percent difference shown in Fig. 5, reveals that the values at 1000 Hz are ≈1.03 for all three functions. That is, the standard accelerometer is 3% higher than the acceleration derived from the Hopkinson bar which agrees with the 3% lower equivalent gage factor derived from the load test. The peak acceleration values for the Hopkinson bar with a gage factor decreased by 3% and for the standard accelerometer are given in Table 1.

The standard accelerometer was calibrated using traceable, fundamental length/time measurements and certified by the Sandia Primary Standards Laboratory. Their estimate of the uncertainty is +5% of reading (File #4092F). Peak acceleration calculated from the bar data agreed with the peak calculated from the standard accelerometer, 1000 Hz, sensitivity within the +5% uncertainty. The differences averaged 4.3% (three standard deviations = 0.6%) at 4,000 *g* and 1.6% (three standard deviations = 1%) at 10,000 and 15,000 *g*. The sum of the standard uncertainty and the maximum of the three standard deviations were added to obtain the estimated uncertainty of 6%. It is felt that the uncertainty should not change as long as the bar suffers no physical damage and the strain gages are not changed.

Table I. Comparison of Corrected Hopkinson Bar Acceleration Values with Standard Accelerometer

Nominal Peak Value (g)	Corrected Hopkinson Bar Peak Acceleration (g)	Standard Peak Acceleration (g)	Percent Difference
4000	4016	4189	4.1
	4233	4425	4.3
	4044	4220	4.2
	4207	4402	4.4
	4042	4237	4.6
10000	10100	10240	1.4
	10180	10380	1.9
	10370	10530	1.5
	10150	10360	2.0
	9825	9977	1.5
15000	16050	16320	1.7
	15680	15930	1.6
	16590	16920	2.0
	14900	15080	1.2
	15860	16040	1.1

CONCLUSIONS

Three characteristics of a 3/4-in. titanium Hopkinson bar were investigated. First, calculations demonstrated that the variation of bar stress wave speed with temperature, for the configuration used to calibrate accelerometers, is negligible. Second, the acceleration derived from a Hopkinson bar was compared to a standard accelerometer with a NIST-traceable calibration, and the variation of the Hopkinson bar response with frequency was characterized. Last, an equivalent gage factor was derived from a calibration of the bar in a load testing machine. The equivalent gage factor is 3% lower than that specified by the manufacturer and agrees with the 3% difference between the standard accelerometer and the Hopkinson bar derived acceleration in the frequency response function calculations at low frequencies. As a result of these investigations, the Hopkinson bar has been certified with an uncertainty of 6%.

This work was supported by the U.S. Department of Energy under Contract DE-AC04-76-DP00789.

REFERENCES

Bateman, V. I., Leisher, W. B., Brown, F. A., and Davie, N. T., 1991, "Calibration of a Hopkinson Bar With a Transfer Standard," *Proceedings of the 62nd Shock and Vibration Symposium,* Springfield, VA, October, 1991, Vol. III, pp. 568–577.

Bendat, J. S., and Piersol, A. G., 1986, *Random Data,* 2nd ed., John Wiley & Sons, New York, pp. 164–185.

Brown, G., 1963, "Accelerometer Calibration With the Hopkinson Pressure Bar," *Instrument Society of America* preprint No. 49.3.63, 18th Annual ISA Conference and Exhibit, September 1963, Chicago, IL.

Cannon, J., and Rimbey, D., 1971, "Transient Method of Calibrating a Piezoelectric Accelerometer for the High g-level Range," *American Society of Mechanical Engineers,* No. 71-Vibr-43, ASME Vibrations Conference and the International Design Automation Conference, September 1971, Toronto, Canada.

Davies, R., 1948, "A Critical Study of the Hopkinson Pressure Bar," *Philosophical Transactions,* Series A, Royal Society of London, Vol. 240, pp. 352–375.

Kolsky, H., 1953, *Stress Waves in Solids,* Oxford University Press, Oxford.

Metallic Materials and Elements for Aerospace Vehicle Structures, June 1987, MIL-HDBK-5E, Section 5.4.1.18.

Sill, R. D., 1983, "Shock Calibration of Accelerometers at Amplitudes to 100,000 g Using Compression Waves," *Proceedings of the 29th International Instrument Symposium,* Albuquerque, NM, May 2–6, 1983, pp. 503–516.

Stearns, S. D., 1975, *Digital Signal Analysis,* Hayden Book Company Inc., pp. 37–40.

Stearns, S. D., 1978, "Integration and Interpolation of Sampled Waveforms," SAND77-1643·UC-32, National Technical Information Service, Springfield, VA.


Journal of Engineering
The Scientific World Journal
International Journal of Rotating Machinery
Journal of Sensors
International Journal of Distributed Sensor Networks
Advances in Civil Engineering
Journal of Control Science and Engineering
Hindawi
Submit your manuscripts at
http://www.hindawi.com
Journal of Robotics
Journal of Electrical and Computer Engineering
Advances in OptoElectronics
VLSI Design
International Journal of Navigation and Observation
Modelling & Simulation in Engineering
International Journal of Aerospace Engineering
International Journal of Chemical Engineering
International Journal of Antennas and Propagation
Active and Passive Electronic Components
Shock and Vibration
Advances in Acoustics and Vibration